ACS APPLIED MATERIALS & INTERFACES

Research Article

www.acsami.org

Electrical Responses of Artificial DNA Nanostructures on Solution-Processed In-Ga-Zn-O Thin-Film Transistors with Multistacked Active Layers

Joohye Jung,[†] Si Joon Kim,[†] Doo Hyun Yoon,[†] Byeonghoon Kim,[‡] Sung Ha Park,*[,‡] and Hyun Jae Kim*[,†]

[†]School of Electrical and Electronic Engineering, Yonsei University, 50 Yonsei-ro, Seodaemun-gu, Seoul 120-749, Republic of Korea

[‡]Department of Physics and SKKU Advanced Institute of Nanotechnology (SAINT), Sungkyunkwan University, Suwon, Gyeonggi-do 440-746, Republic of Korea

ABSTRACT: We propose solution-processed In-Ga-Zn-O (IGZO) thin-film transistors (TFTs) with multistacked active layers for detecting artificial deoxyribonucleic acid (DNA). Enhanced sensing ability and stable electrical performance of TFTs were achieved through use of multistacked active layers. Our IGZO TFT had a turn-on voltage (V_{on}) of −0.8 V and a subthreshold swing (SS) value of 0.48 V/decade. A dry-wet method was adopted to immobilize double-crossover DNA on the IGZO surface, after which an anomalous hump effect accompanying a significant decrease in V_{on} (−13.6 V) and degradation of SS (1.29 V/decade) was observed. This sensing behavior was attributed to the middle interfaces of the multistacked active layers and the negatively charged phosphate groups on the DNA backbone, which generated a parasitic path in the TFT device. These results compared favorably with those reported for conventional field-effect transistor-based DNA sensors with remarkable sensitivity and stability.

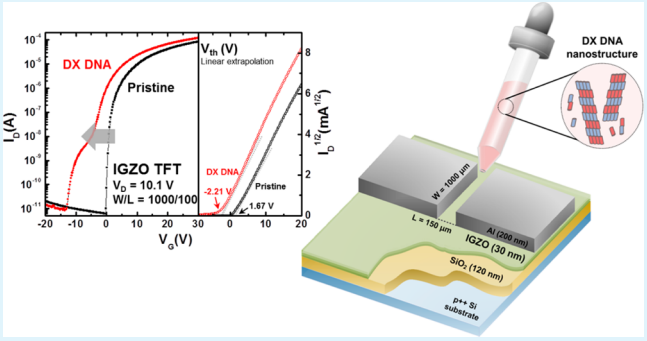

KEYWORDS: *oxide TFTs, biosensors, DNA nanostructure*

1. INTRODUCTION

The detection of nucleic acid targets is becoming increasingly important in human health and safety, particularly with respect to molecular diagnostics, pathogen detection, and anti-bioterrorism strategies.[1−4] In this regard, deoxyribonucleic acid (DNA) biosensors have attracted considerable interest. Although there have been many studies of a variety of DNA biosensors, most rely on the fluorescence detection of labeled probes or targets[2] with the attendant limitations of large and expensive lasers scanners, restricted field deployability, and limited sensitivity. This led to the development of label-free methods, for instance, electrochemical detection,[3,4] atomic force microscopy,[5] micro-cantilever analysis,[6] and field-effect transistor (FET)[7,8]-based DNA biosensors. In particular, FET-based DNA biosensors have been studied intensively, because of their various advantages, including high sensitivity and direct transduction.[8,9] Metal oxide-based thin-film transistors (TFTs) are promising candidates, becaue of their low production costs, high reliability, and easy reproducibility.[10,11]

In previous work, we described solution-processed In-Ga-Zn-O (IGZO) TFTs as alternative DNA biosensors for the first time and manifested that they possessed acceptable sensing capability.[11] Although these results demonstrated the feasibility of metal oxide-based TFTs as DNA biosensors, IGZO TFTs still have some inherent issues in this area. One of these drawbacks is that the excessively high sensitivity of IGZO TFTs causes ambiguous electrical responses for solvents, detected DNA, and external noise. In addition, the unpassivated active layer on which the target would be detected is structurally vulnerable. This exposed oxide layer can be easily contaminated, which inevitably leads to reduction of lifetime and sensing ability of these DNA biosensors. In this paper, we introduce solution-processed IGZO TFTs with multistacked active layers to compensate for these limitations when used as DNA biosensors. We investigated the immobilization of artificial DNA on the multistacked metal oxide channel surface, paying special attention to the stable sensing ability and the sensing mechanism related to the multistacked structure.

2. EXPERIMENTAL PROCEDURE

Indium nitrate hydrate ($In(NO_3)_3{\cdot}xH_2O$), gallium nitrate hydrate ($Ga(NO_3)_3{\cdot}xH_2O$), and zinc acetate dihydrate ($Zn(CH_3COO)_2{\cdot}2H_2O$) were used as precursors to prepare the IGZO solution. The precursors were dissolved in 2-methoxyethanol (2ME) solvent. Monoethanolamine (MEA) was then added as a stabilizer to ameliorate the solubility of the precursors, and acetic acid (CH_3COOH) was added in a dropwise manner to achieve a homogeneous solution. The mixture was stirred for 1 h at 60 °C, after which a 0.1 M solution of IGZO was prepared.

Received: October 4, 2012
Accepted: December 4, 2012
Published: December 4, 2012

As depicted in Figure 1, we fabricated a bottom-gate, top-contact type of TFT structure to evaluate the sensing ability. A heavily doped

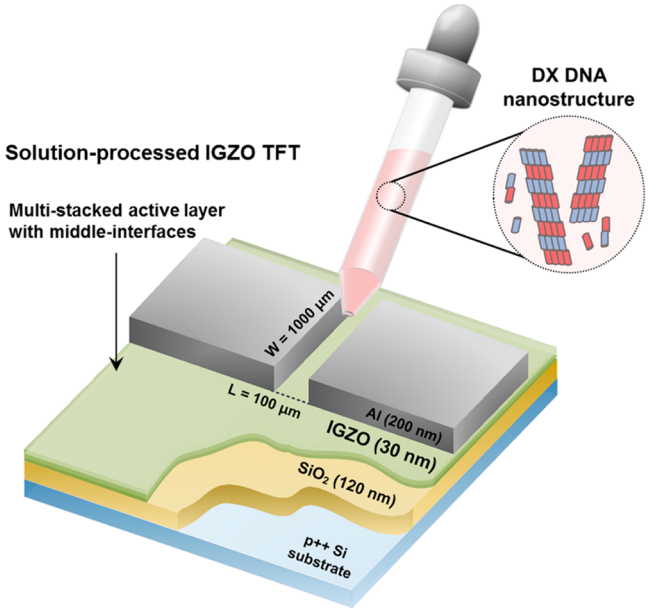

Figure 1. Schematic drawings of solution-processed IGZO TFT structure with multistacked active layer and immobilization of DX DNA nanostructure on the IGZO channel surface.

p-type Si wafer with a thermally grown SiO_2 layer (1200 Å thick) was used as the device substrate. The substrate was cleaned via a standard cleaning method and spin-coated with IGZO solution at 3000 rpm for 30 s, followed by 5 min of pre-annealing at 300 °C and 1 h of annealing at 450 °C in ambient air. This spin-coating and annealing sequence was repeated three times to create the multistacked active layer. Finally, Al was deposited for the source and drain electrodes by sputtering to produce a channel with a length (L) of 100 μm and a width (W) of 1000 μm.

Testing was performed using an artificially designed double-crossover (DX) DNA nanostructure,[12] which means the DNA is manufactured for technical use. This allows accurate control of the analyte for use in a sensor. The construction process of DNA nanostructure is called "free-solution annealing".[11,13] During this procedure, highly selective binding due to complementary base sequences of DNA strands mixed with a water-based physiological buffer, 1 × TAE/Mg^{2+}, which is a mixture of Tris-acetate–ethylenediaminetetraacetic acid (TAE), 40 mM Tris-base, 1 mM EDTA (pH 8.0), and 12.5 mM $Mg(acetate)_2$ provoked the large-scale formation of two-dimensional (2-D) DNA nanostructures. The term "DX" implies that these nanostructures are a group of bridged DX tile units. The tiles consist of four DNA strands forming two duplexes, which are connected by two crossover junctions. Because a single DX tile encompasses 37 base pairs with 3.5 full turns, the length and width of it is 14 nm and 4 nm, respectively. The adjusted concentration of DX monomers was 200 nM, a monolayer of which can fully cover the detection area.[11,14] The synthesized DX DNA was restored and delivered in a non-aqueous solvent, ethanol, using the dry–wet method (DWM), which minimizes the possible detriment of the TFT devices during DNA immobilization.[11,15,16] The detailed procedure of DWM was described in our previous study.[11] The prepared DNA solution was dropped onto the exposed IGZO channel using a micropipet, and the device was then kept in ambient air to allow physical immobilization of the DX DNA nanostructure. For comparison, IGZO TFT upon which ethanol mixed with the buffer solution (i.e., solvent) had been added dropwise was also kept under the same condition.

3. RESULTS AND DISCUSSION

Figure 2 shows the temporal variations of transfer characteristics of the solution-processed IGZO TFTs with multistacked

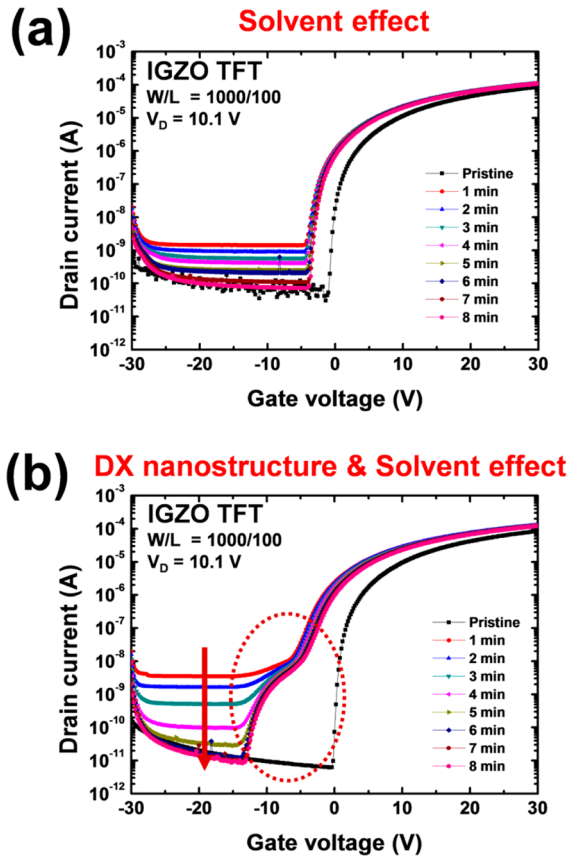

Figure 2. Temporal variation of transfer characteristics of the IGZO TFT exposed to (a) solvent and (b) solvent with DX DNA immobilization.

active layers that confirmed each step of the recovery process after exposure to solvent with and without DX DNA. We measured the electrical characteristics of the devices in darkness under ambient conditions, using a semiconductor parameter analyzer (Model HP4156C; Hewlett Packard, Palo Alto, CA). Note that the device treated with solvent that did not contain DX DNA exhibited a sufficient recovery of the off current (I_{off}) and almost no change in the on current (I_{on}), compared to those devices with a solvent that contained immobilized DX DNA. In particular, the solvent-dropped TFT showed increased I_{off} in the range of 10^{-5}–10^{-3} μA, which dissipated after 8 min when most of the solvent had evaporated, as depicted in Figure 2a. These results clearly indicated that the solvent caused almost no performance degradation of the device except for the turn-on voltage (V_{on}). The slight shift of V_{on} from −1.4 V to −4.4 V that occurred in this case was not observed in unalloyed ethanol pipetted IGZO TFTs in our earlier study.[11] We attribute this shift to the effect of another factor: the residual buffer solution. Although further studies are required to determine the precise mechanism, the buffer solution probably donated additional carriers and caused the negative shift.[17] In this respect, the negative shift of V_{on} without any change in the sub-threshold swing (SS) should be eliminated from the signal of the sensor, indicating the presence of DX DNA.

dx.doi.org/10.1021/am302210g | ACS Appl. Mater. Interfaces 2013, 5, 98–102

On the other hand, a very significant negative shift of V_{on} with an unusual hump was observed in the device treated with immobilized DX DNA, as shown in Figure 2b. The recovery of I_{off}, as a result of solvent evaporation, also occurred. However, the hump characteristic became more apparent, rather than less apparent, after 8 min. Figure 3 shows a detailed analysis of the

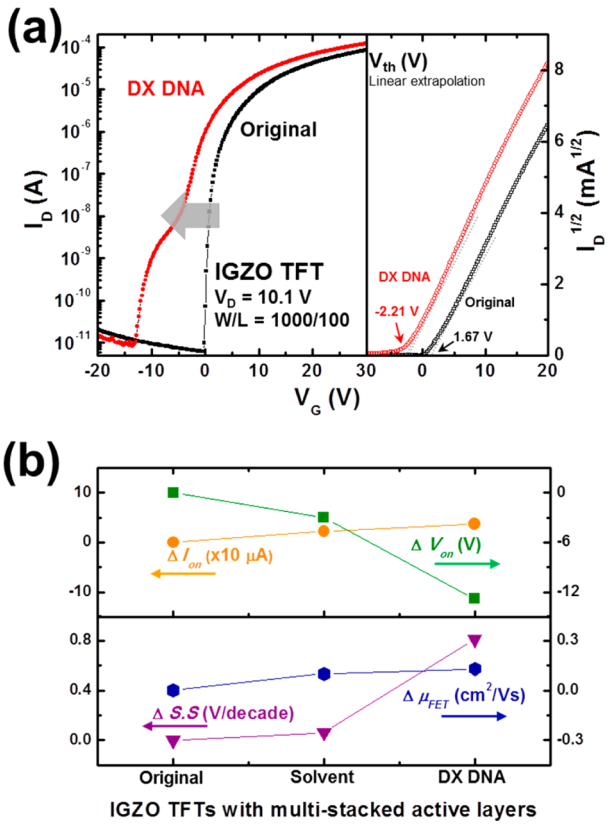

Figure 3. (a) Transfer characteristics of the solution-processed IGZO TFTs with multistacked active layers before and after DX DNA immobilization; (b) variation in turn-on current (I_{on}), turn-on voltage (V_{on}), subthreshold swing (SS), and field-effect mobility (μ_{FET}).

effect of DX DNA immobilization, compared with the pristine device. As indicated in the figure, I_{on} and V_{on} of the original IGZO TFT were 84.73 μA and −0.8 V, respectively, and these values changed to 121.36 μA and −13.6 V, respectively, after DX DNA immobilization. Although these transitions were noticeable, careful analysis is warranted, because they were also affected by solvent, as mentioned above. Simultaneously, an enormous increase in the SS value from 0.48 V/decade to 1.29 V/decade was exhibited, which had been fixed in the case of solvent-dropped device. Conceptually, SS is the required gate voltage corresponding to the factor-of-10 increase in the drain current (I_D) in the sub-threshold region. In this respect, the distinctive change in SS was associated with the exceptional hump behavior of IGZO TFTs with multistacked active layers. In addition, the threshold voltage (V_{th}) was estimated by linear extrapolation of the square root of I_D versus the gate voltage (V_G) at the maximum gradient. A negative shift of the V_{th} value, from 1.67 V to −2.21 V, was observed after DX DNA immobilization. Table 1 summarizes all of these parameter variations.

According to previous literature, the hump in TFTs has been reported in various cases. Uchida et al.[18] and Shur et al.[19] have

Table 1. Comparison of the Electrical Characteristics of Solution-Processed IGZO TFTs with Multistacked Active Layers before and after DX DNA Immobilization

parameter	without DX DNA	with DX DNA
field-effect mobility, μ_{FET}	1.00 cm^2/(V s)	1.13 cm^2/(V s)
on-current, I_{on}	84.73 μA	121.36 μA
turn-on voltage, V_{on}	−0.8 V	−13.6 V
threshold voltage, V_{th}	1.67 V	−2.21 V
subthreshold swing, SS	0.48 V/decade	1.29 V/decade

underlined that gate bias stress causes this hump behavior in amorphous silicon TFTs. They observed that it is concerned with the localized states in back channel interface, comparing the results of experimental measurements and a 2-D device simulator. On the other hand, some studies have shown that the structural factor is also responsible for the hump phenomenon. For instance, it is suggested that the corner parasitic transistor with lower V_{th} derived from corner edges of channel can be triggered before the main transistor.[20] More recently, such a curve seems to be the combination of a dominant transistor and a parasitic transistor, as a result of structural or environmental factors that promote charge trapping in metal oxide-based TFTs.[21−23] Figure 4 shows

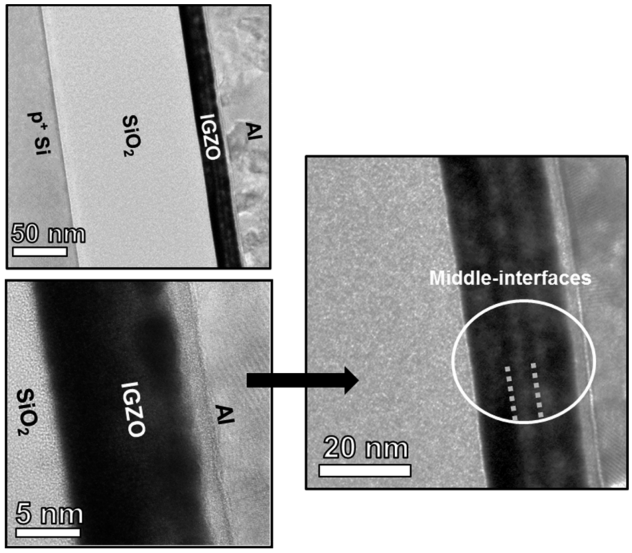

Figure 4. Cross-sectional HR-TEM images of solution-processed IGZO TFTs with multistacked active layers.

cross-sectional high-resolution transmission electron microscopy (HR-TEM) images of IGZO TFT with multistacked layers captured to investigate the novel sensing mechanism, which is different from that used in our earlier work. The multistacked active layer is composed of distinct parts, i.e., stacked layers and the middle interfaces between them, which were formed during the multideposition process and are clearly visible in these images. We interpreted the unusual sensing response of our TFT as being due to the influence of these middle interfaces. Although the middle interfaces are not clearly understood, some studies have suggested that the trap sites in the middle interfaces contribute to the capture of free carriers developing a negative charge barrier and eventually attenuate the gate electric field.[24−26]

We reported previously that the DNA detection mechanism, using IGZO TFTs, is strongly related to electrostatic

dx.doi.org/10.1021/am302210g | ACS Appl. Mater. Interfaces 2013, 5, 98−102

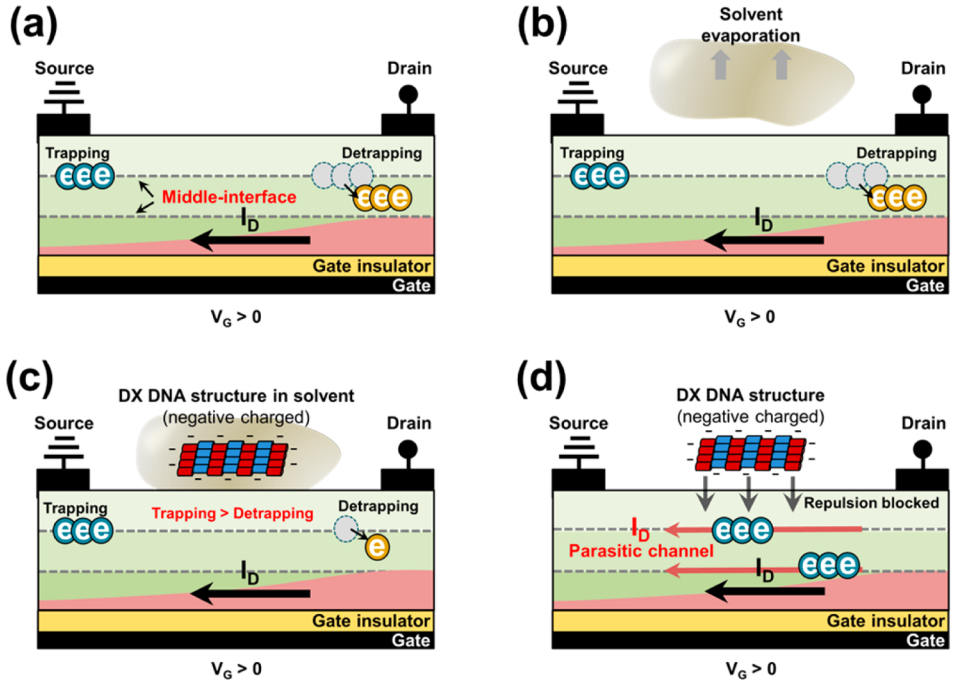

Figure 5. Schematic diagram of the solution-processed IGZO TFTs with multistacked active layers (a) before solvent effect and (b) after solvent evaporation; DNA detection mechanism (c) under solvent effect and (d) after solvent evaporation.

interactions caused by negatively charged phosphate groups of the DNA backbone. As a consequence, this electrostatic repulsion causes electrons to scatter and leads to a decrease in I_D.[11] This process can be interpreted using a second-order differential equation of Poisson, although it requires further study.[27] On the other hand, Figures 5c and 5d depict a somewhat different detection mechanism involving the multistacked active layer structure. Because of the charge barriers of the middle interfaces, the repulsive force of the DX DNA nanostructure is weakened, indicated by the lack of an apparent decrease in I_D. Note that these charges remain trapped in the middle interfaces because of the electrostatic attraction of the immobilized DX DNA. When sufficient charges have accumulated to form a sub-current path or parasitic channel, the device turns on earlier than it would in its normal on-state.[28−30] This procedure results in a hump of the DX DNA immobilized device, which becomes more distinct as the solvent evaporates, as shown in Figure 5d. As mentioned previously, the shifts of SS and V_{th} are subsidiary responses of the hump. For comparison, Figures 5a and 5b show the normal on-state of the pristine device and the effects of solvent without DX DNA, respectively.

Consequently, because of the multistacked active layers, IGZO TFT containing immobilized DX DNA exhibited a transfer curve that was significantly distinguishable from those of the original device or that exposed to solvent. Inserting multistacked active layers guarantees improved sensitivity without any confusing signals, because of the solvent effect. In addition, TEM images showed that the multistacked IGZO layer was much denser than the conventional IGZO layer (data not shown). It is well-known that the relatively high density of the active layer indicates superior thermal or environmental stability with fewer defects.[31] This would extend the lifespan of a biosensor handicapped by an unpassivated active layer for detection.

4. CONCLUSION

In summary, we have demonstrated that solution-processed IGZO TFTs with multistacked active layers show promise as DNA detectors with improved performance, compared to standard IGZO TFTs. The DX DNA nanostructure was immobilized on the IGZO channel surface using the dry−wet method. After DNA adsorption, a significant increase in SS and a negative shift of V_{on} with an accompanying hump were observed in the transfer curve. The obvious changes in electrical parameters were attributed to the multistacked active layer and its middle interfaces. Furthermore, the compact IGZO layer resulting from the multideposition process ensured device stability.

AUTHOR INFORMATION

Corresponding Author

*E-mail addresses: hjk3@yonsei.ac.kr (H.J.K.)p; sunghapark@skku.edu (S.H.P.).

Notes

The authors declare no competing financial interest.

ACKNOWLEDGMENTS

This work was supported by the National Research Foundation of Korea (NRF) grant funded by the Korean Ministry of Education, Science and Technology (MEST) (No. 2011-0028819).

REFERENCES

(1) Debouck, C.; Goodfellow, P. N. *Nat. Genet.* **1999**, *21*, 48−50.
(2) DeRisi, J. L.; Iyer, V. R.; Brown, P. O. *Science* **1997**, *278*, 680−686.
(3) Boon, E. M.; Salas, J. E.; Barton, J. K. *Nat. Biotechnol.* **2002**, *20*, 282−286.
(4) Zhang, J.; Song, S.; Wang, L.; Pan, D.; Fan, C. *Nat. Protoc.* **2007**, *2*, 2888−2895.
(5) Wang, J.; Bard, A. J. *Anal. Chem.* **2001**, *73*, 2207−2212.

(6) Shekhawat, G.; Tark, S.-H.; Dravid, V. P. *Science* **2006**, *311*, 1592−1595.
(7) Sorgenfrei, S.; Chiu, C.-Y.; Gonzalez, R. L.; Yu, Y.-J., Jr.; Kim, P.; Nuckolls, C.; Shepard, K. L. *Nat. Nanotechnol.* **2011**, *6*, 126−132.
(8) Zhu, Q.; Xing, F.; Liu, C.; Hu, Y.; Liu, N.; Wang, J. *Appl. Phys. Lett.* **2011**, *99*, 073301.
(9) Yan, F.; Mok, S. M.; Yu, J.; Chan, H. L. W.; Yang, M. *Biosens. Bioelectron.* **2009**, *24*, 1241−1245.
(10) Reyes, P. I.; Ku, C. J.; Duan, Z.; Lu, Y.; Solanki, A.; Lee, K. B. *Appl. Phys. Lett.* **2011**, *98*, 173702.
(11) Kim, S. J.; Kim, B.; Jung, J.; Yoon, D. H.; Lee, J.; Park, S. H.; Kim, H. J. *Appl. Phys. Lett.* **2012**, *100*, 103702.
(12) Winfree, E.; Liu, F.; Wenzler, L. A.; Seeman, N. C. *Nature* **1998**, *394*, 539−544.
(13) Shin, J.; Kim, J.; Amin, R.; Kim, S.; Kwon, Y. H.; Park, S. H. *ACS Nano* **2011**, *5*, 5175−5179.
(14) Kim, S.; Kim, J.; Qian, P.; Shin, J.; Amin, R.; Ahn, S. J.; LaBean, T. H.; Kim, M. K.; Park, S. H. *Nanotechnology* **2011**, *22*, 245706.
(15) Lee, K. W.; Kim, K. M.; Lee, J.; Amin, R.; Kim, B.; Park, S. K.; Lee, S. K.; Park, S. H.; Kim, H. J. *Nanotechnology* **2011**, *22*, 375202.
(16) Lee, J.; Amin, R.; Kim, B.; Ahn, S. J.; Lee, K. W.; Kim, H. J.; Park, S. H. *Soft Matter* **2012**, *8*, 619−622.
(17) Chung, W.-F.; Chang, T.-C.; Li, H.-W.; Chen, C.-W.; Chen, Y.-C.; Chen, S.-C.; Tseng, T.-Y.; Tai, Y.-H. *Electrochem. Solid State Lett.* **2011**, *14*, H114−H116.
(18) Nishida, S.; Takechi, K.; Hirano, N.; Uchida, H. *J. Non-Cryst. Solids* **1993**, *164*, 755−758.
(19) Slade, H.C.; Shur, M.S. *IEEE Trans. Electron Devices* **1998**, *45*, 1548−1553.
(20) Hatzopoulos, A. T.; Arpatzanis, N.; Tassis, D. H.; Dimitriadis, C. A.; Templier, F.; Oudwan, M.; Kamarinos, G. *IEEE Trans. Electron Devices* **2007**, *54*, 1265−1269.
(21) Tsai, C.-T.; Chang, T.-C.; Chen, S.-C.; Lo, I.; Tsao, S.-W.; Hung, M.-C.; Chang, J.-J.; Wu, C.-Y.; Huang, C.-Y. *Appl. Phys. Lett.* **2010**, *96*, 242105.
(22) Huang, C.-F.; Peng, C.-Y.; Yang, Y.-J.; Sun, H.-C.; Chang, H.-C.; Kuo, P.-S.; Chang, H.-L.; Liu, C.-Z.; Liu, C.W. *IEEE Electron Device Lett.* **2008**, *29*, 1332−1335.
(23) Furuta, M.; Kamada, Y.; Kimura, M.; Hiramatsu, T.; Matsuda, T.; Furuta, H.; Li, C.; Fujita, S.; Hirao, T. *IEEE Electron Device Lett.* **2010**, *31*, 1257−1259.
(24) Kwon, D. W.; Kim, J. H.; Chang, J. S.; Kim, S. W.; Kim, W. D.; Park, J. C.; Song, I. H.; Kim, C. J.; Jung, U. I.; Park, B. G. *Appl. Phys. Lett.* **2011**, *98*, 063502.
(25) Oh, H.; Ko Park, S.-H.; Hwang, C.-S.; Yang, S. H.; Ryu, M. K. *Appl. Phys. Lett.* **2011**, *99*, 022105.
(26) Kim, D. J.; Kim, D. L.; Rim, Y. S.; Kim, C. H.; Jeong, W. H.; Lim, H. S.; Kim, H. J. *ACS Appl. Mater. Interfaces* **2012**, *4*, 4001−4005.
(27) Nair, P. R.; Alam, M. A. *Nano Lett.* **2008**, *8*, 1281−1285.
(28) Huang, S.-Y.; Chang, T.-C.; Chen, M.-C.; Chen, S.-C.; Tsai, C.-T.; Hung, M.-C.; Tu, C.-H.; Chen, C.-H.; Chang, J.-J.; Liau, W.-L. *Electrochem. Solid State Lett.* **2011**, *14*, H177−H179.
(29) Estrada, M.; Cerdeira, A.; Iñiguez, B. *Microelectron. Reliab.* **2012**, *52*, 1342−1345.
(30) Mativenga, M.; Seok, M.; Jang, J. *Appl. Phys. Lett.* **2011**, *99*, 122107.
(31) Li, C.-S.; Li, Y.-N.; Wu, Y.-L.; Ong, B.-S.; Loutfy, R.-O. *J. Mater. Chem.* **2009**, *19*, 1626−1634.